

Electron Hopping Conductivity and Vapor Sensing Properties of Flexible Network Polymer Films of Metal Nanoparticles

Francis P. Zamborini,[†] Michael C. Leopold, Jocelyn F. Hicks, Pawel J. Kulesza,[‡] Marcin A. Malik,[§] and Royce W. Murray*

Contribution from the Kenan Laboratories of Chemistry, University of North Carolina, Chapel Hill, North Carolina 27599-3290

Received February 18, 2002

Abstract: Films of monolayer protected Au clusters (MPCs) with mixed alkanethiolate and ω -carboxylate alkanethiolate monolayers, linked together in a network polymer by carboxylate-Cu²⁺-carboxylate bridges, exhibit electronic conductivities (σ_{EL}) that vary with both the numbers of methylene segments in the ligands and the bathing medium (N₂, liquid or vapor). A chainlength-dependent swelling/contraction of the film's internal structure is shown to account for changes in σ_{EL} . The linker chains appear to have sufficient flexibility to collapse and fold with varied degrees of film swelling or dryness. Conductivity is most influenced (exponentially dependent) by the chainlength of the nonlinker (alkanethiolate) ligands, a result consistent with electron tunneling through the alkanethiolate chains and nonbonded contacts between those chains on individual, adjacent MPCs. The σ_{EL} results concur with the behavior of UV-vis surface plasmon adsorption bands, which are enhanced for short nonlinker ligands and when the films are dry. The film conductivities respond to exposure to organic vapors, decreasing in electronic conductivity and increasing in mass (quartz crystal microgravimetry, QCM). In the presence of organic vapor, the flexible network of linked nanoparticles allows for a swelling-induced alteration in either length or chemical nature of electron tunneling pathways or both.

Introduction

Substantial interest exists in the electronic properties of nanometer-scale materials—carbon nanotubes,¹ fullerenes,² conjugated molecular “wires”,³ semiconductor nanoparticles,⁴ nanowires,⁵ clusters,⁶ and clusters of clusters⁷—with respect both to their fundamental importance and to possible applications in

molecular³ and nanoelectronics.⁸ Synthesis, assembly, alignment, and interconnection of such materials, as well as methods of measuring their electronic properties, are crucial facets of this growing field. Likewise valuable are systematic ways to alter the *iR* electronic properties, including exploiting them for chemical sensing applications.

This paper reports on the electronic conductivity properties of network polymer films of Au₁₄₀ nanoparticles. The individual nanoparticles are coated with mixed monolayers of alkanethiolate (*nonlinker ligands*) and ω -carboxyalkanethiolate (*linker ligands*), and the nanoparticles are linked together⁹ by carboxylate-Cu²⁺-carboxylate coordinative couplings. Scheme 1 shows the different combinations of methylene chainlengths used as linker and nonlinker ligands and the metal ion linking chemistry. We find that the nanoparticle film electronic conductivities are sensitive to both ligand chainlengths and the medium (liquid or vapor) bathing the films. The sensitivity is interpreted to reflect the inherent flexibility of the linker ligand structures and consequent solvent swelling of the network film. In air-dried films, the linker ligand structures seem substantially folded and electron hopping between the Au₁₄₀ cores of the nanoparticles can be demonstrated to occur by nonbonded contacts of nonlinker ligands. Solvation and swelling of the network

* Address correspondence to this author. Email: rwm@email.unc.edu.

[†] Present address: Department of Chemistry, University of Louisville, Louisville, KY 40292.

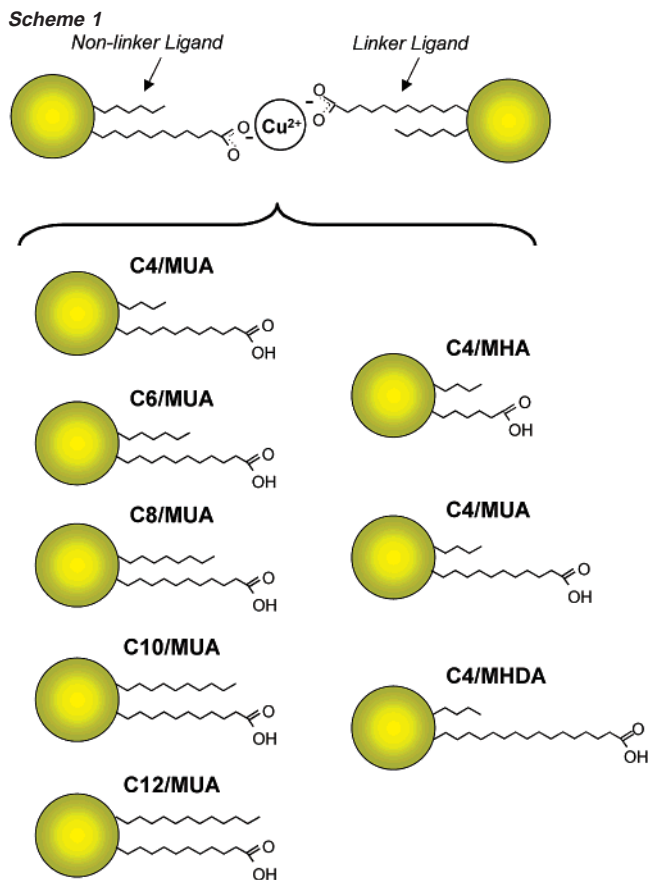
[‡] On leave from University of Warsaw, Department of Chem., Pasteura 1, PL-02-093, Warsaw, Poland, and Technical University of Czestochowa, Division of Chemistry, Al. Armii Krajowej 19, PL-42-200, Czestochowa, Poland.

[§] On leave from University of Warsaw, Department of Chem., Pasteura 1, PL-02-093, Warsaw, Poland, and Technical University of Czestochowa, Division of Chemistry, Al. Armii Krajowej 19, PL-42-200, Czestochowa, Poland.

- (1) (a) Derycke, V.; Martel, R.; Appenzeller, J.; Avouris, Ph. *Nano Lett.* **2001**, *1*, 453–456. (b) Bachtold, A.; Hadley, P.; Nakanishi, T.; Dekker, C. *Science* **2001**, *294*, 1317–1320. (c) Postma, H. W. C.; Teepen, T.; Yao, Z.; Grifoni, M.; Dekker, C. *Science* **2001**, *293*, 76–79.
- (2) (a) Joachim, C.; Gimzewski, J. K. *Chem. Phys. Lett.* **1997**, *265*, 353–357. (b) Ami, S.; Joachim, C. *Nanotechnology* **2001**, *12*, 44–52.
- (3) Tour, J. M. *Acc. Chem. Res.* **2000**, *33*, 791–804.
- (4) (a) Kim, S. H.; Markovich, G.; Rezvani, S.; Choi, S. H.; Wang, K. L.; Heath, J. R. *Appl. Phys. Lett.* **1999**, *74*, 317–319. (b) Jiang, P.; Liu, Z.-F.; Cai, S.-M. *Surf. Sci.* **2001**, *486*, L507–L512.
- (5) (a) Cui, Y.; Lieber, C. M. *Science* **2001**, *291*, 851–853. (b) Kovtyukhova, N. I.; Martin, B. R.; Mbindyo, J. K. N.; Smith, P. A.; Razavi, B.; Mayer, T. S.; Mallouk, T. E. *J. Phys. Chem. B* **2001**, *105*, 8762–8769.
- (6) (a) Simon, U. *Adv. Mater.* **1998**, *10*, 1487–1492. (b) Sato, T.; Ahmed, H.; Brown, D.; Johnson, B. F. G. *J. Appl. Phys.* **1997**, *82*, 696–701. (c) Schmid, G.; Liu, Y.-P.; Schumann, M.; Raschke, T.; Radehaus, C. *Nano Lett.* **2001**, *1*, 405–407. (d) Schmid, G.; Hornyak, G. L. *Curr. Opin. Colloid Interface Sci.* **1997**, *2*, 204–212.
- (7) Feldheim, D. L.; Keating, C. D. *Chem. Soc. Rev.* **1998**, *27*, 1–12.

(8) Joachim, C.; Gimzewski, J. K.; Aviram, A. *Nature* **2000**, *408*, 541–548.

(9) (a) Zamborini, F. P.; Hicks, J. F.; Murray, R. W. *J. Am. Chem. Soc.* **2000**, *122*, 4514–4515. (b) Wuelfing, W. P.; Zamborini, F. P.; Templeton, A. C.; Wen, X.; Yoon, H.; Murray, R. W. *Chem. Mater.* **2001**, *13*, 87–95. (c) Hicks, J. F.; Zamborini, F. P.; Osisek, A. J.; Murray, R. W. *J. Am. Chem. Soc.* **2001**, *123*, 7048–7053. (d) Templeton, A. C.; Zamborini, F. P.; Wuelfing, W. P.; Murray, R. W. *Langmuir* **2000**, *16*, 6682–6688.



polymer film upon contact by an organic liquid or vapor degrades these contacts and diminishes the film's electronic conductivity. The effect is reversible, which suggests a potentiality of these nanoparticle network polymers for chemical vapor sensing.

The gold nanoparticles employed are referred¹⁰ to as monolayer protected clusters (MPCs), a notation continued here to emphasize the stabilizing aspect of the thiolate ligand shells. Electronic communication between the metal-like MPC cores occurs by electron hopping (self-exchange), with the intervening monolayer coatings serving as tunneling bridges. This electronic communication has been investigated¹¹ via the electronic conductivities of cast, non-networked films of arylthiolate and of alkanethiolate-coated MPCs. In the latter case, using MPCs having reasonably monodisperse Au core sizes with observable quantized double layer charging properties,¹² the cast films could be prepared^{11a} with well-defined mixtures of different core electronic "charge states". The ensuing electronic conductivity shows that (a) the electron hopping is a bimolecular process (b) with an extremely fast rate constant that (c) varies exponentially with the core–core spacing as anticipated¹¹ for

an electron tunneling reaction. The large rate constants and small activation barriers are consistent with Marcus relationships^{11a} and, in summary, arise from the low dielectric medium surrounding the Au core reaction centers and the large size of those centers.

We have also investigated the electronic communication between MPC cores in nanoparticle polymer films in which their monolayers have been networked together.^{9c} An electrochemical investigation^{9c} of Au₁₄₀ nanoparticles having mixed monolayers of hexanethiolate and 11-mercaptoundecanoic acid linked by metal ion-carboxylate coordinative coupling, produced 10⁶ s⁻¹ nanoparticle-nanoparticle electron-transfer rate constants. This rate of electron transfer seemed too large to be rationalized by electron tunneling through the very long –SC10CO₂CuCO₂–C10S– linker ligand bridges. These nanoparticle films were contacted by CH₂Cl₂/electrolyte solutions. The present results show that thermal motions of the linker bridges and of the nanoparticles within the solvent-swollen linked network must have allowed electron tunneling to follow shorter reaction pathways, such as through the *nonbonded* –SC6/C6S– contacts.

Films of materials whose electronic conductivities vary with chemical environment, notably vapors, are classically called "chemiresistors".¹³ Carbon particles¹⁴ embedded in polymers are an important example. There have been several¹⁵ chemiresistor studies of MPC films. MPCs, however, do not have a high thermal tolerance,^{11b,16} meaning the use of elevated temperatures during film preparation is inadvisable.^{15a} MPC films with networked films are tolerant to immersion in liquids (that would otherwise solubilize their monomeric constituents) as well as to vapors. There have been no prior studies of the mechanistic aspects of MPC film responses to organic vapors.

Experimental Section

Chemicals. All chemicals were reagent grade and used as received.

Synthesis and Preparation of Mixed Monolayer MPCs. Alkanethiolate monolayer protected clusters (MPCs) were synthesized using a modified Brust reaction.¹⁷ Briefly, butanethiol (C4), hexanethiol (C6), octanethiol (C8), decanethiol (C10), or dodecanethiol (C12) were combined in toluene in a 3:1 mole ratio with AuCl₄⁻, followed by a 10-fold excess of reductant (NaBH₄ in water) at 0 °C. The MPC product was recovered from the stirred reaction mixture after 24 h by precipitation, filtering, and thorough washing with acetonitrile on a glass fritted Buchner funnel. We label this 28 kDa product¹⁸ as C_n MPC, where *n* is the number of carbons in the alkanethiolate chain.

Linker ligands (6-mercaptohexadecanoic acid (HS(CH₂)₅CO₂H, MHA), 11-mercaptoundecanoic acid (HS(CH₂)₁₀CO₂H, MUA), and 16-mercaptohexadecanoic acid (HS(CH₂)₁₅CO₂H, MHDA) were place-exchanged¹⁹ for some of the *nonlinker* C_n ligands in the initial MPC

- (10) (a) Hostetler, M. J.; Murray, R. W. *Curr. Opin. Colloid Interface Sci.* **1997**, *2*, 42. (b) Templeton, A. C.; Wuelfing, W. P.; Murray, R. W. *Acc. Chem. Res.* **2000**, *33*, 27.
- (11) (a) Wuelfing, W. P.; Green, S. J.; Pietron, J. J.; Cliffel, D. E.; Murray, R. W. *J. Am. Chem. Soc.* **2000**, *122*, 11465–11472. (b) Terrill, R. H.; Postlethwaite, T. A.; Chen, C.-C.; Poon, C.-D.; Terzis, A.; Chen, A.; Hutchison, J. E.; Clark, M. R.; Wignall, G.; Londono, J. D.; Superfine, R.; Falvo, M.; Johnson, C. S.; Samulski, E. T.; Murray, R. W. *J. Am. Chem. Soc.* **1995**, *117*, 12537–12548.
- (12) (a) Chen, S.; Ingram, R. S.; Hostetler, M. J.; Pietron, J. J.; Murray, R. W.; Schaaff, T. G.; Khoury, J. T.; Alvarez, M. M.; Whetten, R. L. *Science* **1998**, *280*, 2098. (b) Chen, S.; Murray, R. W.; Feldberg, S. W. *J. Phys. Chem. B* **1998**, *102*, 9898. (c) Hicks, J. F.; Templeton, A. C.; Chen, S.; Sheran, K. M.; Jasti, R.; Murray, R. W. *Anal. Chem.* **1999**, *71*, 3703.

- (13) Janata, J. *Principles of Chemical Sensors*; Plenum Press: New York, 1989.
- (14) Albert, K. J.; Lewis, N. S.; Schauer, C. L.; Sotzing, G. A.; Stitzel, S. E.; Vaid, T. P.; Walt, D. R. *Chem. Rev.* **2000**, *100*, 2595–2626.
- (15) (a) Wohltjen, H.; Snow, A. W. *Anal. Chem.* **1998**, *70*, 2856–2859. (b) Evans, S. D.; Johnson, S. R.; Cheng, Y. L.; Shen, T. *J. Mater. Chem.* **2000**, *10*, 183–188. (c) Han, L.; Daniel, D. R.; Maye, M. M.; Zhong, C.-J. *Anal. Chem.* **2001**, *73*, 4441–4449.
- (16) Hostetler, M. J.; Wingate, J. E.; Zhong, C.-J.; Harris, J. E.; Vachet, R. W.; Clark, M. R.; Londono, J. D.; Green, S. J.; Stokes, J. J.; Wignall, G. D.; Glish, G. L.; Porter, M. D.; Evans, N. D.; Murray, R. W. *Langmuir* **1998**, *14*, 17–30.
- (17) Brust, M.; Fink, J.; Schiffrin, D. J.; Kiely, C. *J. Chem. Soc., Chem. Commun.* **1995**, 1655–1656.
- (18) (a) Whetten, R. L.; Khoury, J. T.; Alvarez, M. M.; Murthy, S.; Vezmar, I.; Wang, Z. L.; Stephens, P. W.; Cleveland, C. L.; Luedtke, W. D.; Landman, U. *Adv. Mater.* **1996**, *8*, 428. (b) Ingram, R. S.; Hostetler, M. J.; Murray, R. W.; Schaaff, T. G.; Khoury, J. T.; Whetten, R. L.; Bigioni, T. P.; Guthrie, D. K.; First, P. N. *J. Am. Chem. Soc.* **1997**, *119*, 9279–9280.
- (19) Hostetler, M. J.; Templeton, A. C.; Murray, R. W. *Langmuir* **1999**, *15*, 3782.

monolayer. Stirring tetrahydrofuran (THF) solutions of MPC and linker ligand (in selected molar ratios) for ca. 4 days gave mixed monolayer MPCs that were collected and washed as above. The mole ratio of linker to nonlinker thiolates was determined by NMR of solutions of the disulfides that were quantitatively liberated from the mixed monolayer MPCs upon decomposition with iodine.¹⁹

On the basis of transmission electron microscopy (TEM) and thermogravimetry as described previously,¹⁶ the C_n MPCs have average core diameters of 1.6 ± 0.8 nm and $Au_{140}(Cn)_{53}$ composition. The MPCs with mixed monolayers containing MUA have (by NMR) the average composition $Au_{140}(Cn)_{33}(MUA)_{20}$. The compositions are averages in that a dispersion of Au core sizes exists (as determined by TEM). Additionally, some dispersity in the C_n/MUA ligand ratio is statistically expected within the overall MPC population.

Formation and Electronic Conductivities of Network MPC Films.

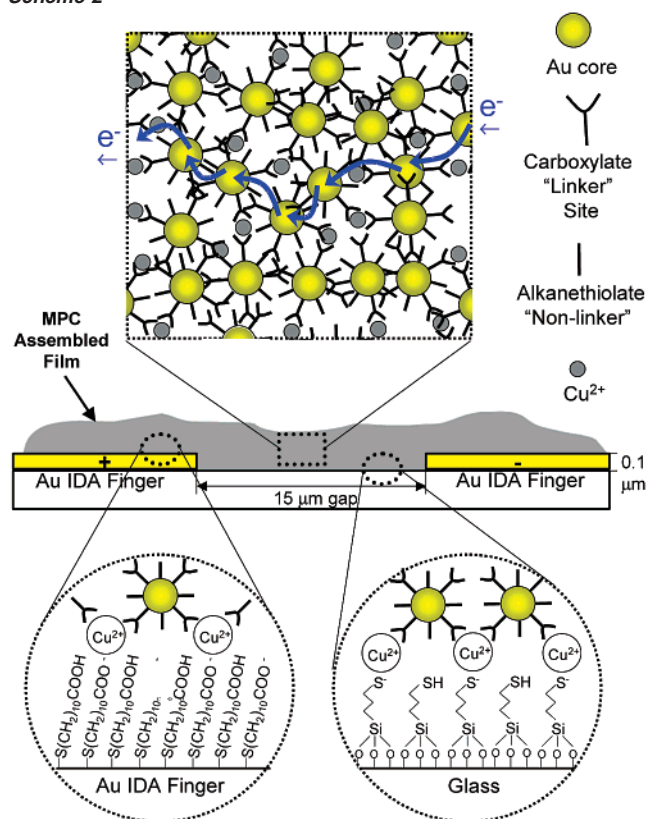
Solid-state electronic conductivity measurements were made on nanoparticle network polymer films attached to interdigitated array electrodes (IDAs, Microsensor Systems, Inc). The IDAs consist of 50 interdigitated Au fingers (4800 μm long, 15 μm wide, 0.1 μm high) deposited on glass and separated by 15 μm gaps (d_G). The Au fingers are treated as parallel plate electrodes of total area^{11a} $A_{\text{total}} = A_{\text{finger}}(N - 1) = 4.8 \times 10^{-6}$ cm^2 , where $N = 50$ and A_{finger} is finger length \cdot height. The IDA geometric cell constant [d_G/A_{total}] is 6.3 cm^{-1} . The areas of the top faces of the IDA fingers are ignored since very little current is probably passed between these faces and the area comprising the ends of each finger is considered negligible. Wire leads were attached to the IDA contact pads with Ag epoxy (cured 48 h, 100 $^\circ\text{C}$), which was insulated with an overlayer of torr-seal epoxy (cured 10 h, 100 $^\circ\text{C}$). The IDA was cleaned in boiling toluene (10–15 min), rinsed with acetone and ethanol, and dried under N_2 .

The IDAs were chemically treated with the goal of attaching an initial MPC layer to both the Au fingers and SiO_2 gaps, to promote uniform MPC film growth. A layer of 3-mercaptopropyltrimethoxy silane (MPTMS)²⁰ was attached to the glass gap surface by exposing the IDA to 100 μL of MPTMS in 10 mL of 2-propanol (plus 2–3 drops deionized water) and heating to near boiling for 30 min. The IDA was rinsed with ethanol, dried under a N_2 stream, and heated at 100 $^\circ\text{C}$ for 5–10 min. The IDA was again ethanol rinsed, and its Au fingers were derivatized by exposure to 2 mM mercaptoundecanoic acid (MUA) in ethanol (15 min), forming a COOH-terminated self-assembled monolayer (SAM).²¹ Scheme 2 shows a cartoon of the thusly treated IDA finger and gap surfaces.

The films were assembled using previously described⁹ copper(II)-carboxylate coordination, for example, as follows for $Au_{140}(Cn)_{33-n}(MUA)_{20}$ MPCs where $n = 4, 6, 8, 10,$ or 12 (see Scheme 1). The treated IDA was serially exposed to 0.1 M $\text{Cu}(\text{ClO}_4)_2 \cdot 6\text{H}_2\text{O}$ in ethanol (10 min), rinsed with ethanol, exposed to 1–2 mg/mL MPC in ethanol²² (30 min), rinsed with ethanol, and then dried under N_2 . This protocol, a “dip cycle”, deposits several monolayers of MPC.⁹ Additional dip cycles serve to build up the network film thickness. A similar procedure was employed to form C_n films possessing linker ligands of mercaptohexanoic acid (MHA) and mercaptohexadecanoic acid (MHDA).

The quantity of MPCs deposited on the IDAs was monitored⁹ spectrophotometrically at 520 nm (ATI Unicam spectrometer) using glass slides that had been subjected to an identical series of dip cycles,

Scheme 2



continuing them until the slide's absorbance (A) = 0.8 ± 0.2 . Using a constant MPC surface coverage ensures that variations in conductivity due to different populations of electron hopping centers between the IDA fingers are minimized. Based on $\epsilon_{\text{Au}_{140}} \approx 4 \times 10^5 \text{ M}^{-1} \text{ cm}^{-1}$, $A = 0.8$ corresponds to an MPC surface coverage of $2.1 \times 10^{-9} \text{ mol/cm}^2$ or ca. 140 monolayers of MPC at $1.5 \times 10^{-11} \text{ mol/cm}^2$ for a cubic lattice-packed MPC monolayer. The physical thicknesses of the MPC films is less readily monitored; we estimate film thicknesses ranging from 0.2 to 2 μm depending on the nonlinker chainlength and various assumptions about swelling and chain interdigitation.^{11,23} These estimated thicknesses all exceed the 0.1 μm IDA finger height.

MPC film conductivity, $\sigma_{\text{EL}} = d_G \Delta i / A_{\text{total}} \Delta E$, was obtained from the slope $\Delta i / \Delta E$ (in the linear response range, ± 200 mV) of current–potential responses to ± 1.0 V potential sweeps (100 mV/s, PAR model 273 potentiostat). Changes in film conductivity (200 mV potential bias, model CHI 660A electrochemical workstation, CH-Instruments) upon exposure to ethanol vapor were measured by alternately exposing the IDA to dry N_2 and to N_2 /ethanol vapor mixtures (using flow rate controllers) ranging from 0 to 100% room-temperature partial pressures.

Quartz Crystal Microbalance. The vapor phase partition of ethanol into MPC network films was assessed by weighing the films using quartz crystal microbalance (QCM) methods.²⁴ MUA self-assembled monolayers were deposited on the 1.13 cm^2 gold films on polished 5 MHz AT cut crystals (Maxtek, Inc.), and MPC films were deposited on them using the IDA procedure. The crystals were mounted in the same flow cell as used for the conductivity measurements and alternately exposed to dry N_2 and ethanol vapors as above. QCM frequency changes were measured using a home-built instrument and a HP 53131A universal counter interfaced to a PC with Labview 4.0 software. The Sauerbrey equation with integral sensitivity, $C_F = 56.6 \text{ Hz cm}^2 \mu\text{g}^{-1}$, was used to relate frequency changes²⁴ to mass changes.

(23) Luedtke, W. D.; Landman, U. *J. Phys. Chem. B* **1998**, *102*, 6566–6572.

(24) Buttry, D. A.; Ward, M. D. *Chem. Rev.* **1992**, *92*, 1355–1379.

(20) Goss, C. A.; Charych, D. H.; Majda, M. *Anal. Chem.* **1991**, *63*, 85–88.

(21) (a) Ulman, A. *An Introduction to Ultrathin Organic Films from Langmuir–Blodgett to Self-Assembly*; Academic Press: San Diego, 1991. (b) Ulman, A. *Chem. Rev.* **1996**, *96*, 1533–1554.

(22) The MPC concentrations slightly varied for different chainlengths depending on the solubility of the MPC in ethanol. Generally, 40 mg was dissolved in 10 mL of ethanol and filtered through glass wool and a syringe filter to remove insoluble clusters. Another 10 mL of ethanol was added, and the solution was split into two vials each containing 10 mL. One vial was used for depositing the MPC film onto an IDA, and the second vial was used for deposition onto a similarly treated glass slide, which was used to monitor film growth by UV–vis spectroscopy.

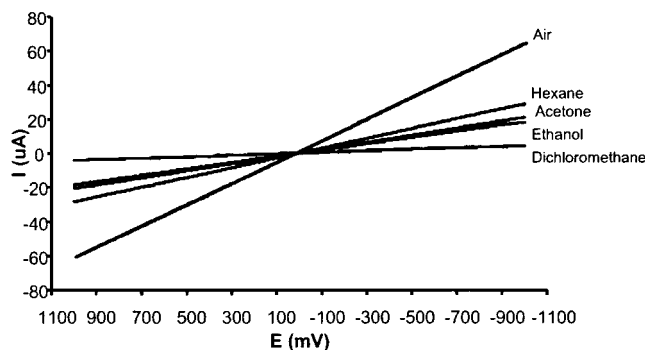


Figure 1. I–E curves of a C6/MUA film in air ($\sigma_{\text{EL}} = 3.9 \times 10^{-4} \Omega^{-1} \text{cm}^{-1}$) and immersed in various liquids, including hexane ($\sigma_{\text{EL}} = 1.8 \times 10^{-4} \Omega^{-1} \text{cm}^{-1}$), acetone ($\sigma_{\text{EL}} = 1.3 \times 10^{-4} \Omega^{-1} \text{cm}^{-1}$), ethanol ($\sigma_{\text{EL}} = 1.1 \times 10^{-4} \Omega^{-1} \text{cm}^{-1}$), and dichloromethane ($\sigma_{\text{EL}} = 2. \times 10^{-5} \Omega^{-1} \text{cm}^{-1}$).

Results and Discussion

The nanoparticle films in this study were prepared from 1.6 nm (av) diameter Au MPCs containing mixed monolayers (Scheme 1) of alkanethiolates [$\text{S}(\text{CH}_2)_n\text{CH}_3$] and carboxylic acid terminated alkanethiolates [$\text{S}(\text{CH}_2)_n\text{COOH}$]. We have previously described both the assembly⁹ of the network films, using coordinative carboxylate/ Cu^{2+} /carboxylate bridges, and the two anchoring chemistries^{9a–c} (see Scheme 2) that graft the films onto the Au finger and silica gap parts of the IDAs. Repeated “dipping cycles” were employed to deposit network nanoparticle films so that they contained, according to their optical absorbances (see Experimental Section), roughly equal surface coverages of MPCs. Eliminating film thickness effects permits a focus on how the monolayer architecture of the MPCs and their network linking chemistry influence the dynamics of MPC core-to-core electron hopping. The electronic conductivity of the nanoparticle films occurs by electron hopping between MPC cores, which as discussed above occurs by tunneling reactions through the intervening monolayer structures.

If a network polymer film of C6/MUA MPC nanoparticles (see Scheme 1) on an IDA is exposed to an ion-free bathing environment, such as air or a pure *nonionic* solvent, smooth current–potential responses (Figure 1) result from applying a potential bias between the IDA fingers. These responses reflect electronic conductivity supported by electron hopping (Scheme 2, not to scale). The absence of hysteresis in the I–V response shows that there is no significant mass transport of ions internal to the nanoparticle films and no electrolytic double layer charging at the film/IDA electrode interfaces, at least on these experimental time scales.

It is obvious from Figure 1 that the network nanoparticle polymer film’s electronic conductivity (σ_{EL} is the slope of the current–potential curve near its origin; see figure legend for values) varies strongly with the nature of the bathing medium. The conductivity, which is proportional^{11,25} to the rate of electron hopping, is large when the film is exposed to ambient laboratory air but drops by over 10-fold when the film is immersed in various organic solvents. The responses shown were stable to repeated potential sweeping, and the nanoparticle film could

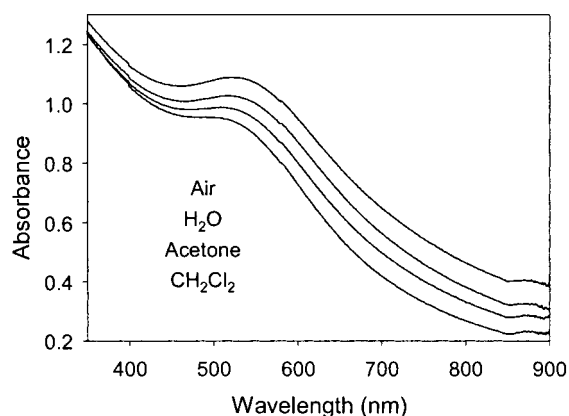


Figure 2. UV–vis spectra of a C4/MUA MPC film on glass in various solvents. In air, the film shows a surface plasmon band at 550 nm. Immersing the film in organic solvents such as acetone and CH_2Cl_2 red-shifts the band position and (relative to air) decreases the intensity of the band, as a result of film swelling. The change in the surface plasmon is less in a polar solvent such as water because the film is fairly hydrophobic.

be repeatedly immersed in pure solvent and air-dried without noticeable degradation of the σ_{EL} response in either solvent or air. The inference of the variations in conductivity with bathing medium is that either the length or chemical nature (or both) of electron tunneling pathways can be varied by solvent partition from the bathing medium into the nanoparticle film.

That changes in nanoparticle separation distances accompany changes in bathing medium is qualitatively supported by electronic spectra of a C4/MUA nanoparticle film deposited on glass (Figure 2). It is well-known²⁶ that the ca. 520 nm surface plasmon absorption band of Au particles is enhanced and red-shifted when the particles become aggregated or otherwise pushed closer together. We have, for example, noticed⁹ that the normally barely detectable plasmon band of dissolved Au_{140} nanoparticles becomes readily observable when the MPCs are assembled (and thus concentrated) into a network polymer film. Figure 2 shows that the plasmon band of the C4/MUA MPC film is more prominent in air relative to that in CH_2Cl_2 solvent. The film conductivities of Figure 1 fall in a similar order, being largest in air and smallest in CH_2Cl_2 solvent. It is plausible from this comparison that variations in nanoparticle spacing are provoked by partitioning of organic solvent into the film, thereby swelling it. Swelling is especially expected in CH_2Cl_2 vapor because the nanoparticles are quite soluble in liquid CH_2Cl_2 . Conversely, drying the film causes collapse to a more concentrated MPC structure.

While conductivity change with solvent swelling might be interpreted as simply reflecting changes in electron tunneling distances, the factors that control the rate of electron hopping are likely to be much more complex. For example, the network of ligands linking the film together is probably more disordered than ordered, so that electron tunneling occurs over a distribution of pathways and core–core distances. For significant conductivity to exist, however, the aggregate population of electron tunneling pathways must lie above a percolation threshold. Additionally, the thermal motions of nanoparticle sites about equilibrium positions in solvent-swollen polymers may vary substantially with local, solvent-influenced microscopic viscosity. It follows then that nanoparticle film swelling will not necessarily alter conductivity on simply distance-related grounds.

(25) (a) Sosnoff, C. S.; Sullivan, M.; Murray, R. W. *J. Phys. Chem.* **1994**, *98*, 13643. (b) Terrill, R. H.; Hutchinson, J. E.; Murray, R. W. *J. Phys. Chem. B* **1997**, *101*, 1535. (c) Ritchie, J. E.; Murray, R. W. *J. Am. Chem. Soc.* **2000**, *122*, 2964. (d) Dickinson, E.; Masui, H.; Williams, M. E.; Murray, R. W. *J. Phys. Chem. B* **1999**, *103*, 11028. (e) Masui, H.; Long, J. W.; Malik, J.; Murray, R. W. *J. Am. Chem. Soc.* **1997**, *119*, 1997.

(26) Quinten, M.; Kreibitz, U. *Surf. Sci.* **1986**, *172*, 557–577.

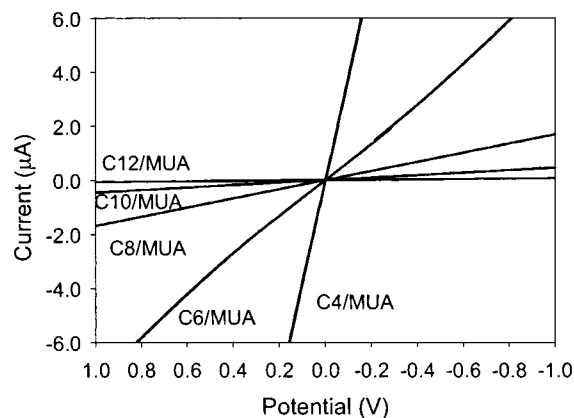


Figure 3. Current–potential responses (± 1.0 V) of various C_n /MUA MPC films deposited onto IDA electrodes, obtained in air at 100 mV/s. Higher slopes between ± 200 mV are indicative of more conductive films. See Table 1 for the average results.

Table 1. Electronic Conductivities of Network Nanoparticle Films^a

nonlinker/linker ligand in MPC monolayer ^b	electronic conductivity, σ_{EL} ($\Omega^{-1} \text{ cm}^{-1}$)
C4/MUA	2×10^{-4}
C6/MUA	7×10^{-5}
C8/MUA	9×10^{-6}
C10/MUA	2×10^{-6}
C12/MUA	5×10^{-7}
C4/MHA	5×10^{-3}
C4/MHDA	4×10^{-4}

^a Average results for ≥ 1 films. ^b MHA \equiv mercaptohexanoic acid; MUA \equiv mercaptoundecanoic acid; MHDA \equiv mercaptohexadecanoic acid.

Changes in Electron Hopping Rates in Dry Films with Ligand Chainlength (σ_{EL}). The relation of monolayer structure to air-dry nanoparticle network polymer film conductivity was explored by varying the lengths of the methylene chain segments of both linker and nonlinker ligands. Figure 3 shows conductivity results for air-dried nanoparticle films of MPCs having various nonlinker chainlengths (C4/MUA, C6/MUA, C8/MUA, C10/MUA, and C12/MUA, see Scheme 1). Figure 3 is an important result, showing that large changes in conductivity, and thus electron hopping rates, can occur in films in which the linker ligand structure is *constant*. Clearly, and as was speculated in our previous report,^{9c} the linker ligand is not the primary electron tunneling pathway in the network polymer. Instead, we see that the efficacy of electron hopping (tunneling) varies by nearly 10^3 -fold with the chainlength of the *nonlinker* ligand and is largest for the shortest nonlinker ligand. The conductivity measurements are summarized in Table 1.

The Figure 3 conductivity results are consistent with the behavior of the surface plasmon absorbance shown in Figure 4. The collective resonance effect of increasing MPC core proximity is greatest for the shortest nonlinker ligand chainlengths. The collective band at 550 nm is also more pronounced when the film is in air rather than in a solvent (Figure 2), as discussed above. In contrast, the spectra of all of these MPCs dissolved in solution are substantially featureless, as reported before.¹⁶

Experiments where the nonlinker methylene chainlength was held constant at C4 and that of the linker ligand was varied over C5, C10, and C15 are shown in Figure 5. These films are coded in the results as C4/MHA, C4/MUA, and C4/MHDA, respectively. The conductivities of these films decrease in the

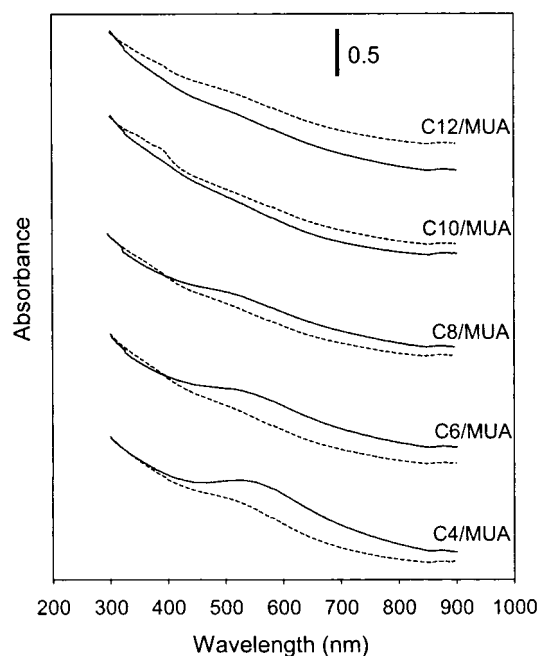


Figure 4. UV–vis spectroscopy of C_n /MUA MPCs (dashed lines) in ethanol solution and (solid lines) assembled in films on glass slides using carboxylate– Cu^{2+} –carboxylate bridges. The spectra in solution (dashed lines) are featureless or show minor surface plasmon bands, but the spectra of the films (solid lines) show an enhanced band near 550 nm especially for the shorter chainlengths, presumably due to the close spacing of the gold cores. Spectra are offset for comparison (absorbance at 300 nm is 1.3–1.5 in all cases).

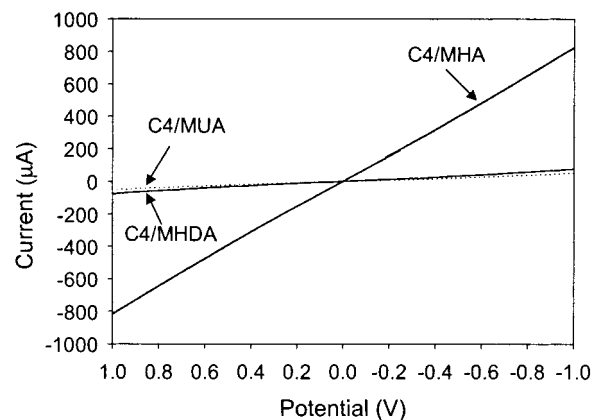


Figure 5. Current–potential responses (± 1.0 V) of C4 MPC films attached by linkers of different chainlengths (MHA, MUA, MHDA) obtained in air at 100 mV/s. Higher slopes between ± 200 mV are indicative of more conductive films. See Table 1 for average results.

order given (Table 1), with the C4/MHA film being much more conductive than the others. The difference in conductivity between the C4/MUA and C4/MHDA is much less than that which might be expected were tunneling to occur *solely* through the linker chains.

We attempted to construct a similar series of nanoparticle films in which the linker ligand chainlength was long and that of the nonlinker ligand was varied. Films with short nonlinker ligands (C4/MHDA and C6/MHDA) exhibited large σ_{EL} , consistent with the preceding. However, reliable deposition of films with nonlinker ligands containing ≥ 8 methylene units proved to be difficult, and results with such films were compromised owing to variations in nanoparticle film thicknesses.

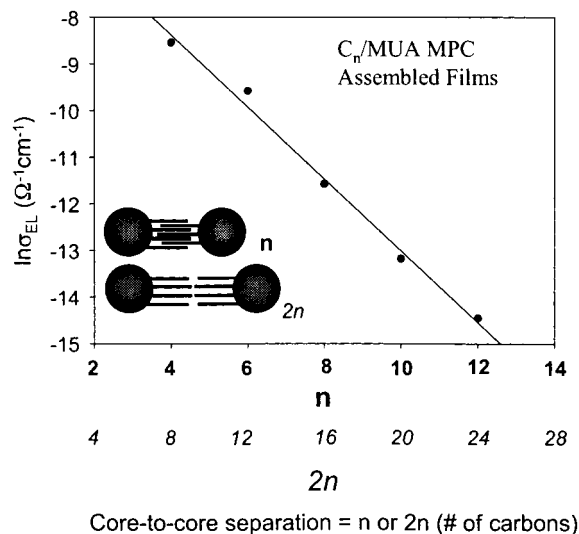


Figure 6. Plot of $\ln \sigma_{EL}$ for the C_n/MUA films vs average Au MPC separation in terms of number of carbons (z). Depending on the packing arrangement within the film, z is shown as either n (bold) for full interdigitation or $2n$ (italics) for no interdigitation, where n is the total number of carbons in the nonlinker alkane chain. β values for the fully interdigitated film and the noninterdigitated film are 0.8/carbon and 0.4/carbon, respectively.

Demonstration of Electron Tunneling in Dry Films. The principal signature of an electron transfer that occurs by a tunneling mechanism is an exponential dependency of its rate on the distance of tunneling (or the number of methylene units in tunneling bridge chain). Figure 3 showed (see above) that the chainlength of the nonlinker ligands on the MPCs has a major effect on the network polymer film's electronic conductivity. Figure 6 displays the conductivities from Figure 3 as an exponential plot, which is respectably linear. This result is conclusive, showing that electron transfers in dry films occur by tunneling through nonbonded contacts between the *nonlinker* chains. The obvious inference is that the longer, structurally flexible linker ligand is a less efficient tunneling bridge and is folded or coiled to allow the nonbonded nonlinker contacts.

The slope of the Figure 6 tunneling plot is the product of the electronic coupling factor (β) and the tunneling dimension (measured as either distance or number of methylene units). The actual tunneling dimension is unfortunately uncertain, since alkanethiolate ligands on MPCs are known both experimentally¹⁶ and from theory²³ to interdigitate or intercalate with the ligands of adjacent MPCs, to nearly their full length. There is consequent uncertainty in assessing β from the slope of Figure 6, since tunneling distance depends on the packing arrangement of the nonbonded ligands in the films. Interdigitation also appears to occur for the dry, network polymer nanoparticle films. If Figure 5 were interpreted on the basis of electron transfers between methyl–methyl nonbonded tunneling contacts (i.e., $2n$ units in the overall bridge), one obtains $\beta = 0.4 \text{ C}^{-1}$, which is an unrealistically small value. If full nonlinker chain interdigitation were assumed, a value of 0.8 C^{-1} is obtained, which is close to previous results from research on well-ordered self-assembled monolayers.^{11,27,28} Thus, not only does tunneling in dry C_n/MUA network films occur predominantly through the nonlinker ligands, but the structural folding of the linker chains also allows

(27) Smalley, J. F.; Feldberg, S. W.; Chidsey, C. E. D.; Linford, M. R.; Newton, M. D.; Liu, Y.-P. *J. Phys. Chem.* **1995**, *99*, 13141.

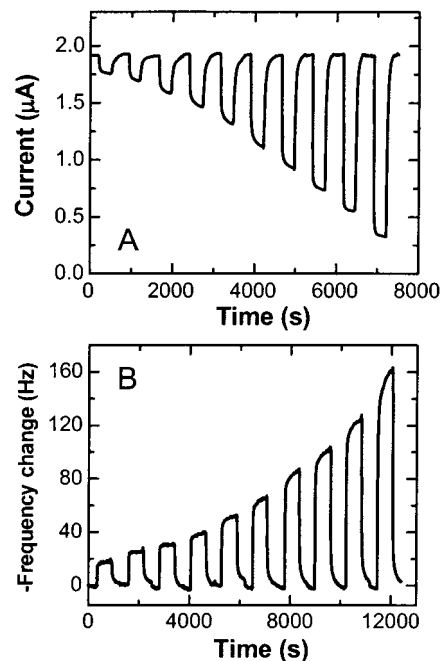


Figure 7. Upon application of a constant potential (-0.2 V) to an IDA electrode modified with an assembled C_6/MUA MPC film, (A) current changes are monitored over time. Films were alternately exposed to pure nitrogen flow and successively increasing ethanol vapor. (B) Identical experiments were performed simultaneously on the same C_6/MUA film formed on a QCM gold substrate. Ethanol vapor partial pressures were successively increased in a sequence of fractions, 0.1, 0.2, 0.3, 0.4, 0.5, 0.6, 0.7, 0.8, 0.9, and 1.0 of the saturated ethanol vapor pressure (7.9 kPa). Baseline responses were recorded in the atmosphere of pure nitrogen purged through the flow system.

the nonlinkers to engage in the van der Waals interactions that promote chain interdigitation to some undetermined extent. This latter result is somewhat surprising, as it implies that the network of bonding connections between linker ligands on adjacent MPCs is not only flexible but quite sparse. That is, only a fraction of the approximately 20 carboxylate sites on each MPC may actually be engaged in linking together the polymeric network.²⁹

The linker chains are, however, not completely lacking in control over the electron hopping dynamics, as seen in Figure 4. Long linker chainlengths yield similar conductivities, but a short linker (e.g., C_4/MHA , Scheme 1) provides substantially higher conductivity. Whether this corresponds to a more extensive interdigitation of the nonlinker C_4 chains or to a more orderly packing with a higher density of MPC-MPC contacts is unclear.

Response to Vapor Exposure. It is obvious from the preceding results that the networked nanoparticle films have possibilities for analytical measurements of organic vapor concentrations, i.e., vapor sensing. Others¹⁵ have also seen this possibility and reported results for different kinds of nanoparticle films. An initial report by Wohltjen and Snow^{15a} examined the vapor response sensitivity, in terms of changing film resistance, of octanethiol modified gold nanoparticle films dropcast onto

(28) (a) Slowinski, K.; Fong, H. K. Y.; Majda, M. *J. Am. Chem. Soc.* **1999**, *121*, 7257–7261. (b) Holmlin, R. E.; Haag, R.; Chabinye, M. L.; Ismagilov, R. F.; Cohen, A. E.; Terfort, A.; Rampi, M. A.; Whitesides, G. M. *J. Am. Chem. Soc.* **2001**, *123*, 5075–5085. (c) Wold, D. J.; Frisbie, C. D. *J. Am. Chem. Soc.* **2001**, *123*, 5549–5556.

(29) There is no information available at present on the dependency of conductivity on number of carboxylate sites.

IDA electrodes (and unfortunately treated at temperatures conducive to decomposition of MPC monolayers and nanoparticle aggregation) and exposed to a variety of different solvent vapors. Evans and co-workers^{15b} investigated the vapor sensing capabilities of films composed of nanoparticles stabilized with small, aromatic organothiol derivatives with a variety of substituted endgroups. While the focus of their study was to look at the role of functional groups in particle–particle interactions, they also explored each type of film’s sensing potential by bathing them in different types of vapor. Core size effects were the focus of a QCM/ σ_{EL} based vapor sensing study by Zhong and co-workers^{15c} utilizing nanoparticles linked with dithiols or hydrogen bonding between carboxylic acid terminated alkanethiols.

The network MPC films investigated here are chemically linked to the electrode contacts and each other. Their responses to exposure to vapors of ethanol or CH_2Cl_2 and nitrogen are rapid, stable, and reversible decreases in film conductivity and increases in mass (by quartz crystal microgravimetry, QCM). Figure 7 shows an illustrative set of results for ethanol vapors taken in a more extensive study that will be presented as a separate report.³⁰ Figure 7A shows changes in the electronic conductivity of a C6/MUA MPC film on an IDA in response to exposure to pure N_2 and to ethanol vapor of successively increased partial pressure. The current changes are measured using a constant potential bias (0.2 V). Figure 7B shows QCM results obtained in the same experiment and in the same flow cell housing the IDA, for a C6/MUA MPC film deposited on a gold covered quartz resonator. Assuming that the Sauerbrey relation²⁴ is applicable for these experiments (see footnote, Table 2), the decrease in QCM frequency corresponds to a proportionate increase in film mass, as ethanol partitions into the

Table 2. Response of Network Nanoparticle Films to Saturated (7.9 kPa) Ethanol Vapor

MPC film	% Δi	$-\Delta f$ (Hz)	ethanol absorbed (nmol) ^a	Δi /response time (s)	QCM response time (s)
C4/MUA	72	150	65	47	192
C6/MUA	75	156	68	8	
C10/MUA	33 ^b	100	43	13 ^b	168
C4/MHA	51 ^b	na	na	9 ^b	na
C4/MHDA	83 ^b	na	na	7 ^b	na

^a Calculated from the Sauerbrey equation, assuming absence of viscoelastic effects. The change in volume upon partitioning of ethanol vapor is estimated to be $\leq 5\%$. Viscoelastic effects, expected to be negligible with these films at low vapor pressures, will be explored further in a subsequent report dedicated to vapor response.^{30,31} ^b Obtained in a different flow cell.

nanoparticle network polymer film. In both sets of results, incremental increases of ethanol partial pressure provoke similarly incremental changes in conductivity and mass of the C6/MUA MPC film. The data of Figure 7 were preceded by a preconditioning of the film by repeated, alternating exposure to ethanol vapor and N_2 , which improves the film’s response reversibility and response time. What occurs during preconditioning is unknown.

Results for the response of network polymer films containing several different combinations of nonlinker and linker chain-length to saturated ethanol vapor are summarized in Table 2. The vapor-induced conductivity changes vary with film structure, and the response time (90% of final response) for current is generally faster than that for mass. The pervasive aspect of the results shown is that changes in conductivity are accompanied by changes in mass, i.e., film swelling leads to diminished rates of electron hopping.

Acknowledgment. This research was supported in part by research grants from the National Science Foundation and the Office of Naval Research.

JA025965S

(30) Kulesza, P. J.; Malik, M. A.; Leopold, M. C.; Hicks, J. F.; Zamborini, F. P.; Murray, R. W. Manuscript in preparation.

(31) Grate, J. W. *Chem. Rev.* **2000**, *100*, 2627–2648.